Nuclear Instruments and Methods in Physics Research B 358 (2015) 179–187

Contents lists available at ScienceDirect

Nuclear Instruments and Methods in Physics Research B

journal homepage: www.elsevier.com/locate/nimb

Why neutron guides may end up breaking down? Some results on the macroscopic behaviour of alkali-borosilicate glass support plates under neutron irradiation

R. Boffy [a], M. Kreuz [a], J. Beaucour [a,*], U. Köster [a], F.J. Bermejo [b]

[a] Institut Laue-Langevin, 71 avenue des Martyrs, CS 20156, F-38042 Grenoble Cedex 9, France
[b] Instituto de Estructura de la Materia, Consejo Superior de Investigaciones Cientificas, Serrano 123, E-20886 Madrid, Spain

ARTICLE INFO

Article history:
Received 15 April 2015
Received in revised form 16 June 2015
Accepted 17 June 2015
Available online 3 July 2015

Keywords:
Neutron guide
Radiation damage
Glass
Neutron instruments

ABSTRACT

In this paper we report on a first part of a study on the mechanisms leading to brittle fracture in neutron guides made of glass as structural element. Such devices are widely used to deliver thermal and cold neutron beams to experimental lines in most large neutron research facilities. We present results on macroscopic properties of samples of guide glass substrates which are subjected to neutron irradiation at relatively large fluences. The results show a striking dependence of some of the macroscopic properties such as density, shape or surface curvature upon the specific chemical composition of a given glass. The relevance of the present findings for the installation of either replacement guides at the existing facilities or for the deployment of instruments for ongoing projects such as the European Spallation Source is briefly discussed.

1. Introduction

Neutron guides are optical components widely installed in large experimental neutron facilities running either static sources such as a nuclear reactor or at accelerator-driven facilities. The surge of such now widespread devices was motivated by two technical reasons, namely to allow the installation of more scientific instruments on a single source and to lower the background noise on experiment's detectors. They are used to transport thermal or cold neutrons to experimental stations that can be positioned several tens of metres away from the neutron production point. They have enabled the technique to significantly widen its scope, allowing the development of a suite of instruments able to tackle problems pertaining to a wide spectrum of disciplines such as condensed matter, neutron and nuclear physics, chemistry, materials science and engineering, bio- and geosciences.

The basic physics behind the operation of a neutron guide was clarified long ago by Hughes and Burgy [1] based upon the principles of neutron total external reflection. The first practical implementation of such a device came a decade later with Maier-Leibnitz and Springer [2] and Alefeld et al. [3]. The guides are usually made of polished flat borosilicate glass coated with metallic nickel or some supermirror multilayer. Typically rectangular shapes are used with dimensions from 100 to 200 mm height and 30 to 60 mm width. For a given guide, the energy selection of the transported neutrons depends on the mirrors m values,[1] its radius of curvature and its width or height whether it is bent horizontally or vertically respectively. The use of a boron-rich glass substrate fulfils two different purposes, first assuring the desired surface quality for the neutron reflecting material and also to absorb the neutrons that are not reflected by the mirror on ^{10}B nuclei. In fact, such glasses show at ambient temperature remarkable thermal and mechanical properties, exhibiting a rather low volume expansion coefficient ($\approx 3 \times 10^{-6}$ K^{-1}), a Young modulus of about 64×10^3 N mm^{-2}, a Poisson ratio of 0.2 and a tensile strength within 35–100 MPa, depending upon composition. Usually the particle transport is done under vacuum which constitutes a source of stress for the guide walls when they are not placed in an evacuated housings. The neutron shielding ability of this type of substrates spare its surrounding environment from being activated.

The motivation behind our efforts comes from episodes of neutron guide failures reported from different facilities [4–7]. Such failures usually result in breakup of the guide structure leading to an implosion due to loss of vacuum and the generation of a pressure wave which may transport relatively large guide debris at

* Corresponding author.
E-mail address: beaucour@ill.fr (J. Beaucour).

[1] The m value of a given mirror is the ratio the maximum Q-value that can be reflected divided by the one of an nickel mirror.

http://dx.doi.org/10.1016/j.nimb.2015.06.017
0168-583X/

speeds of a few tens of metres per second, thus able to cause some significant damage. Neutron guide degradation under flux is a long time struggle for neutron research facilities. In 1978, the ILL experienced some difficulties with in-pile thermal-guide elements,[2] that is it happened less than five years after their installation. At that time, Pyrex glass had been identified as the cause of failure and was then replaced by A8866 from Corning. Later, efforts have been done towards the understanding of the irradiation ageing of neutron supermirrors [8,9]. Finally, the ILL restarted its investigations on this topic following early guide damages that took place on several of its beam lines (H113, H17 and H25).

The origin of these failure episodes was promptly ascribed to radiation damage effects on the glass substrate [10,11]. Within those, radiation resulting from the capture reaction $^{10}B + n \rightarrow {}^{7}Li + \alpha$ was assumed to be the most deleterious. In fact, the cross-section for neutron capture on Boron-10 (20% natural abundance in Boron) is huge (3980 barn) already for neutrons with thermal energies (0.025 eV). For cold neutrons the cross-section is even higher $\sigma \propto 1/\sqrt{(E_n)}$. In 6% of the neutron captures the decay proceeds to the ground state of ^{7}Li while 94% decays proceed via the excited state of ^{7}Li and are accompanied by emission of a 478 keV gamma ray. For both such cases the Q value (i.e the minimum possible energy released) of the reaction is large compared to the incoming neutron energy and the total kinetic energy of the resulting products α and ^{7}Li basically equals the reaction energy. Conservation of energy and momentum gives values of 1.16 MeV for ^{7}Li and 1.78 MeV for the α particle for the ground state reaction and 0.84 MeV for ^{7}Li and 1.47 MeV for α particle generated by the gamma-ray accompanied reaction. Both charged particles have high linear energy transfer and short range, hence deposit their kinetic energy locally within few ten micrometres from the point of capture.

There has been a number of reports on the effects of particle radiation on the properties of borosilicate glasses, although in most cases the studies concentrate on the effects of relatively low doses of electron [12], γ-rays [13], helium [14], heavier atoms [15] and neutrons [16,17]. Also, a significant effort has been devoted towards the understanding of phenomena taking place in glasses employed for nuclear waste confinement [18,19]. The results evidence a modification of the vitreous structure with an evolution of the borosilicate elementary network units coupled with the formation of radiolytic products such as oxygen, phase segregation, formation of voids or gas bubbles and/or migration of hydrogen or the alkali ions as a consequence of radiation-induced diffusion processes. Part of the results here detailed have already been referred to by Beaucour et al. [5,20] as conference presentations but no subsequent archival publication ensued. It has to be mentioned that this issue is of critical importance for the exploitation and renewal of existing experimental facilities that handle thermal or cold neutron beams. Ongoing projects such as the European Spallation Source based upon concepts which are based on rather long neutron guides (many tens of metres) will benefit from the results of this study.

Our aim here is thus to contribute towards the understanding of guide failure due to accumulated neutron dose, seeking to select the most radiation resistant materials which would prolong the lifetime of the guides beyond periods of those commercially available. As a first step, we focus upon the macroscopic phenomena resulting from glass irradiation and how such effects may provide a clue for the rupture of neutron guides when exposed to excessive fluence. In particular, special care is put in quantifying the stress induced by neutron radiation by means of measurements of the curvature of irradiated plates. The relationship of the present findings with observed changes within the glass matrix at the micro- or nano-scales constitutes the topic being actively pursued at the present time.

[2] H2 systems.

2. Materials and methods

2.1. Studied materials

The four studied materials constitute industry-grade alkali borosilicate glass standards, namely Borofloat, N-ZK7, N-BK7 and S-BSL7. The first three are commonly used for neutron guide manufacturing. In all cases the glass samples have been provided by different neutron guide manufacturers. As far as sample sizes are concerned, we have examined two sample types depending upon their thickness. Thicker samples are 9, 11 or 15 mm thick and thin plates have a thickness of 1.1 mm. Table 1 reports their chemical composition and density before irradiation.

2.2. Equipment employed for radiation

Three experimental set ups have been used depending upon the sought effects of neutron irradiation on glasses.

2.2.1. Radiation hardness

To test the radiation hardness, neutron fluxes provided by the H112 and H21 guides have been used. Such devices provide a collimated flux of 6×10^{10} cold neutrons s^{-1} cm^{-2} and 1.1×10^{9} thermal neutrons s^{-1} cm^{-2}, respectively. These flux values have been measured by means of gold foil activation techniques, hence we quote here for cold neutrons, the equivalent thermal neutron capture flux.

The experimental setup described above was built to mimic the configuration which a glass faces when installed within a guide, namely neutron incidence under small angles. The result is that neutrons are stopped in a small layer right under the mirror and induce an heterogeneous dose in the glass substrate. However, and for the sake of reaching a high dose more quickly, a 4.3° average incidence angle was set. The net result of such an arrangement is that all neutrons within the beam will cross through the mirror and penetrate the glass matrix. In comparison, neutrons which are not reflected by the mirror have a maximum angle of about 3° (a typical value for a $m = 2$ cold neutron guide and neutrons with wavelength of 15 Å). Within such an arrangement the maximum flux should be around 1° (m = 2 cold guide and 5 Å neutrons). The relevance and consequences of this set of measurements are discussed in sections below.

A sample holder able to accommodate up to 30 samples set with an average incidence angle of 4.3° was built for the purpose. The frontal irradiation values quoted above yield values for the whole sample surface of 4.5×10^{9} n s^{-1} cm^{-2} and 8.2×10^{7} n s^{-1} cm^{-2} for H112 and H21 respectively. Table 2 summarizes the information regarding the irradiation setups.

The samples were made of 200 mm length and could be up to 15 mm thick. The stack height could reach 108 mm. In total, 80 samples were irradiated for long periods (50 days minimum), a lapse of time set by the reactor cycles, and were extracted during reactor shut-downs to check their surface state. Fig. 1 shows the sample holder fully loaded with pristine samples. For each kind of glass irradiated, three surface states were prepared, namely a surface polished with 600-paper, another polished up to neutron optical quality (<1 μm diamond suspension) and finally a surface similar to that of a real guide, that is having an additional neutron reflective layer.

Table 1
Chemical composition and density of the studied glasses.

Mol.%	Borofloat	N-ZK7	N-BK7	S-BSL7
SiO_2	82	66	73	73.5
B_2O_3	12	11.5	10	9.5
ZnO		10		
Al_2O_3	1.5	4	0.25	
MgO			1.25	
Na_2O	4	7.5	10	10
K_2O	0.5		5	5.5
CaO		1	0.25	
BaO			0.25	0.5
Density (g/cm^2)	2.205	2.469	2.491	2.504

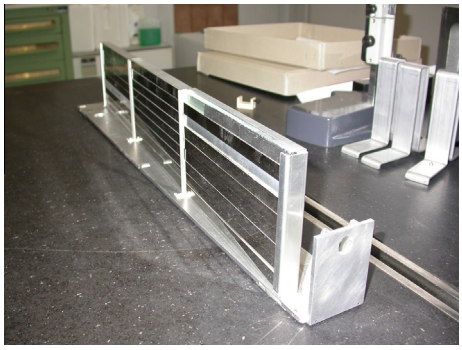

Fig. 1. Sample holder used for irradiation at the H112 and H21 guides.

2.2.2. Homogeneous irradiation

To measure the density evolution of the different glasses upon absorbed neutron dose a setup allowing homogeneous irradiation has been prepared so that thin samples with dimensions $10 \times 10 \times 1.1$ mm (±0.1 mm) could be used. The T4 irradiation tube of the ILL reactor has been chosen for that purpose. This beam tube is located within the reflecting light water vessel, very close to the heavy water tank. Before the experiment, the non-perturbed thermal flux was measured yielding 2×10^{13} n s^{-1} cm^{-2}. The red curve in Fig. 3 displays this flux as a function of the vertical distance from the core median plane. Such a curve has been calculated from results coming from a MCNP [21] computation. Table 3 gathers information concerning the damage induced by the (n,α) reactions in the glass matrix. Due to its high cross section, it represents more than 99.9% of the neutron absorptions in the glass. The reported values have been calculated by SRIM [22] for the most probable case (94%) where the reactions goes through the ^{7}Li excited state. The chosen glass for the calculation is N-ZK7. As the other materials exhibited very similar values, they have not been reported in the article.

Because of the large heat production resulting from the (n,α)-reactions on the ^{10}B nuclei, a new irradiation shuttle had to be designed, since the use of the already existing T4-shuttle would have resulted in samples reaching a temperature above 700 °C. Such temperature would have lead to unwanted annealing phenomena and may have ended up in damage of the aluminium shuttle itself. To remove the heat produced in the glass samples, a thin sample holder was built with two plates wrapping the 1.1 mm thick tiles. The two plates have been vertically rabbeted to enhance the natural water flow. The shuttle has been designed to allow water to fill the voids of the sample cases. For the thermal calculation, we considered a worst case consisting on a stagnation scenario where water was not flowing. The third element of the sample holder is the weighing element which is made to ensure the shuttle dives down to the bottom of the irradiation tube. This new apparatus has been manufactured from AG3net (a variant of the Aluminium alloy AL5754 with reduced contents of the neutron-activating impurities Cu, Zn, etc.) and passivated to comply with the nuclear safety rules of the ILL. Fig. 2 shows a 3D drawing of the irradiation shuttle. There, the orange coloured pieces represent the glass samples. The full capacity of the apparatus is 20 glass samples but for the current experiment only 16 slots have been used. In order to reduce statistical error, for a given glass and irradiation time, four samples were inserted in the shuttle.

Table 2
Numerical values for the incident neutron capture fluxes and fluences for the H112 and H21 irradiation campaign. Values are derived from the gold foil activation measurements.

	Beam flux (n s^{-1} cm^{-2})	Fluence during 50 days reactor cycle (n cm^{-2})
H112 (cold beam)	6×10^{10}	2.6×10^{17}
H21 (thermal beam)	1.1×10^{9}	4.8×10^{15}

In order to carry out a validation of the thermal behaviour of this setup several thermo-hydraulics computations have been carried out. The input heat sources were taken from MCNP and analytic calculation results. The heating in T4 due to nuclear reactions and gamma radiation had already been calculated for a sphere consisting in one gram Aluminium (see the green curve on Fig. 3). A value of 0.17 W/g for the maximum power was assumed for the whole Aluminium shuttle even though its extremities are exposed to lower radiation levels. For the glass samples, in addition, the (n,α) reactions had to be taken into account since they generate an important amount of energy which is trapped within the material as most of it is shared by the ions. The blue curve of Fig. 3 displays such a heat as calculated for N-ZK7 following,

$$P_{^{10}\mathrm{B}(n,\alpha)} = \Sigma_{^{10}\mathrm{B}(n,\alpha)} \cdot \Phi \cdot \frac{Q_{^{10}\mathrm{B}(n,\alpha)}}{1.6 \cdot 10^{-19} \cdot \rho} \quad (1)$$

where $\Sigma_{^{10}\mathrm{B}(n,\alpha)}$ is the thermal macroscopic cross section of the $^{10}\mathrm{B}(n,\alpha)$ reaction. For the computation, a figure for the nuclear heating[3] of 12 W/g was taken for all the samples. Let us mention that such value is to be taken as a realistic upper bound since it does not take into account the sample self-protection and/or the flux reduction due to the presence of absorbing elements.

The results from the computational fluid dynamics can be gauged by inspection of Fig. 4, which displays the maximum temperatures reached by the shuttle loaded with 20 generic borosilicate samples. It can be seen that the maximum temperature is around 63 °C. Such temperature is acceptably low since the glass transition temperature of all four glasses is around 550 °C. Another advantage of the irradiation method here employed concerns the fact the thermal conditions under which the samples are subjected to are comparable to those of a real guide, that is the mirror plates are close to room temperature. It is also worth pointing out that guide heating due to neutron and γ radiations only occur within the first 5 m.

To monitor the flux during the different radiation runs, 99.8% pure Zirconium foils (25 μm thick) were added to each shuttle in order to know the perturbed flux the samples were exposed to [23]. Each foil measured around 4 mm^2 and was wrapped in a larger aluminium foil to block it between a sample and a shuttle plate. These measurements confirmed that the flux, once perturbed by the borosilicate tiles, was noticeably lower than the non-perturbed value and around 7×10^{12} n s^{-1} cm^{-2}. Five batches

[3] By nuclear heating we refer to the heat deposited within the sample as a result of nuclear reactions and γ rays.

Table 3
(n,α) reaction damage in N-ZK7 as calculated by SRIM [22]. The initial energy corresponds to that for the most likely decays which comprise 94% of the reactions.

	Energy (keV)	Ionization stopping		Nuclear stopping		Range (μm)	Induced displacements (ion^{-1})
		$(\frac{dE}{dx})$ (eV/nm)	Fraction (%)	$(\frac{dE}{dx})$ (eV/nm)	Fraction (%)		
α	1.470	<316	99.35	<0.335	0.65	4.7	160
^{7}Li	840	<521	97.2	<1.91	2.8	2.5	400

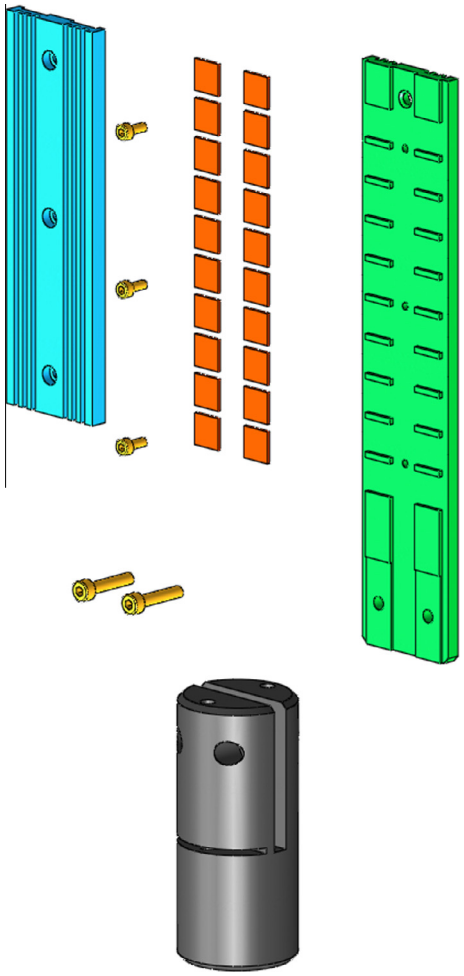

Fig. 2. New irradiation shuttle for the T4 irradiation tube at ILL.

of samples have been irradiated and the received doses are reported in Table 4. The deposited energy by ionization and nuclear interactions, $E_{\text{ioniz.}}$ and $E_{\text{nucl.}}$ respectively, and resulting number of displacements per atom (dpa) have been inferred from Table 3 results.

2.2.3. Glass bending under irradiation

To visualize the generation of stress in the glasses, an irradiation in the Neutrograph test instrument has been carried out [24]. A special sample holder with a capacity of 4 glass plates has been designed for that purpose. The Neutrograph is fed by the H9 thermal neutron beam which has a 3×10^9 n s^{-1} cm^{-2} thermal flux plus a fast neutron component of about 0.1%. Thanks to the sample holder, the mean incidence angle of the neutrons was set to 4.3°. In view of the flux difference of orders of magnitude, the effects of the fast neutrons can be neglected. The advantage of using this equipment for large sample irradiation, compared to H112 or H21, comes from the fact that the samples are available at any time. One only needs to shut-down the H9 beam to enter in the experimental area while it needs to wait for a reactor shut-down in the other case. It allows to choose the total irradiation dose precisely.

2.3. Sample characterization

Four techniques have been used to characterize the samples after their irradiation in the different conditions described earlier.

2.3.1. Splintering detection

The irradiation limit of each glass type has been defined as the neutron fluence at which the glass surface starts to splinter. Such criterion is used at ILL when checking, between two reactor cycles, if an installed guide can be kept or has to be replaced. On such grounds, visual inspection of the plates were carried out at the end of the different reactor cycles. The aim of the measurements was thus to find critical fluence values beyond which the glass plates would break and therefore the neutron guides have to be changed to avoid brittle fracture once such radiation doses are reached.

2.3.2. Density monitoring

To follow the density evolution of the glasses, we have employed the hydrostatic weighting method. A density determination kit has been installed on a Mettler-Toledo AE240 weighting scale. Measurements on the non irradiated samples have shown that this equipment could reach a standard deviation around 0.05% which is low enough considering the expected variations which are one order of magnitude bigger [25].

2.3.3. Curvature measurement

The curvature of thin plates has been measured by a Coordinate Measuring Machine (CMM). This was a Mitutoyo EURO-C-A776 model with Renishaw SP600M measuring tip. To ensure that the plate is not displaced by the tracing pin, a prototype device has been made to press the plate onto the two long sheared edges.

2.3.4. Neutron activation analysis

To understand the different behaviour found for the glass samples here considered and also to quantify the neutron activation of the materials, a set of γ-spectrometry measurements was carried out. Indeed, as this study aims to contribute towards the understanding of the macroscopic behaviour of some alkali borosilicate glasses for future neutron guides, it is important to know the radioactive inventory that is expected when they will be installed within the facility. For this purpose, two high purity germanium detectors have been used; specifically the models Eurisys EGPC 30-185-R and 25-185-R. The same equipment has been used to measure the activity of the Zr foils.

3. Results

3.1. Radiation hardness

The present study allowed us to determine a radiation hardness value for two of the four glasses: Borofloat and N-ZK7. Borofloat shows the lowest value. Due to the relatively high flux in H112, a

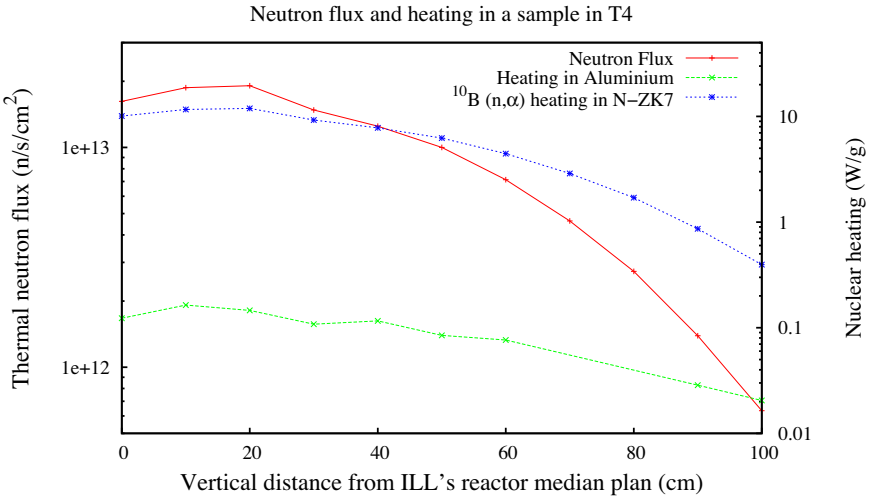

Fig. 3. Flux and nuclear heating in T4 irradiation tube.

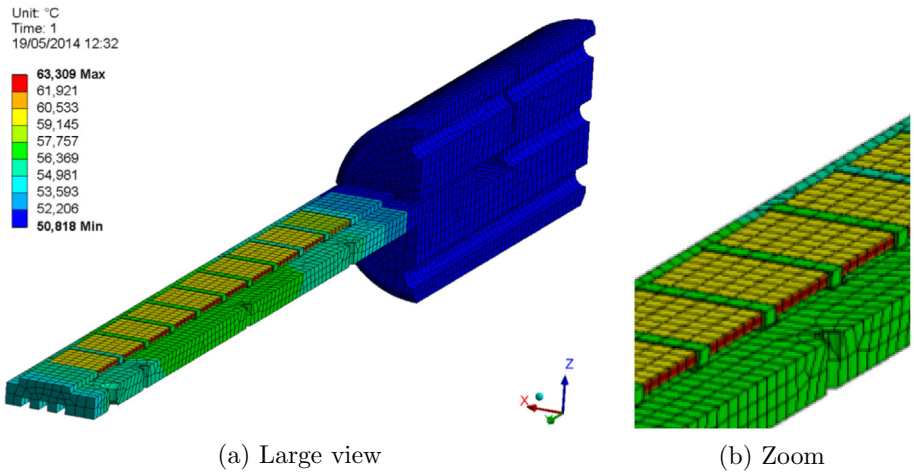

Fig. 4. Computer fluid dynamics calculation showing the maximum temperature reached by the borosilicate glass samples when irradiated in T4. The blue plate from Fig. 2 has not been shown but was, of course part of the simulation. (For interpretation of the references to color in this figure legend, the reader is referred to the web version of this article.)

Table 4
Fluence resulting from homogeneous irradiation and the corresponding deposited energy by ionisation and nuclear interactions. Values derived from Table 3.

Irradiation fluence	1	2	3	4	5
Fluence (n cm^{-2})	$1.3 \cdot 10^{17}$	$2.9 \cdot 10^{17}$	$3.9 \cdot 10^{17}$	$7.6 \cdot 10^{17}$	$2.2 \cdot 10^{18}$
(n,α) reactions (cm^{-3})	$5.1 \cdot 10^{17}$	$1.1 \cdot 10^{18}$	$1.5 \cdot 10^{18}$	$3.0 \cdot 10^{18}$	$8.7 \cdot 10^{18}$
$E_{\text{ioniz.}}$ (keV cm^{-3})	$1.2 \cdot 10^{21}$	$2.6 \cdot 10^{21}$	$3.5 \cdot 10^{21}$	$6.9 \cdot 10^{21}$	$2.0 \cdot 10^{22}$
$E_{\text{nucl.}}$ (keV cm^{-3})	$1.7 \cdot 10^{19}$	$3.8 \cdot 10^{19}$	$5.1 \cdot 10^{19}$	$1.0 \cdot 10^{20}$	$2.9 \cdot 10^{20}$
dpa	0.0041	0.0091	0.012	0.024	0.070

whole reactor cycle brought a beam fluence of 2.6×10^{17} n cm^{-2}. Such radiation dose was large enough to splinter the sample surface irrespective of having a mirror, super-mirror or nothing attached. The ageing experiments in H21 allowed to find an radiation hardness of this material yielding values of $2.8 \times 10^{16} \pm 1 \times 10^{16}$ n s^{-1} cm^{-2}, beam fluence. In consequence, we see that this material is difficult to use in a neutron guide near a primary source and should be relegated to guide sections located behind choppers, velocity selectors or monochromators. As an example of a broken glass plate, Fig. 5 displays an irradiated Borofloat sample, showing its irradiated surface splintered like mosaic. Also notice the high optical density shown by an initially transparent glass due to the formation of colour centers in very large numbers. The fluence limits for the different glasses are summarized in Table 5.

3.2. Density measurements

The density variation of the different glasses with received dose is displayed in Fig. 6. The error bars shown in the figure display the standard deviation calculated from the measured values. Also, for each sample, at least four weighings have been done in order to ensure the reproducibility. One can see from the graph that Borofloat is the sample most affected by radiation. In fact, its density increases up to 2% for a fluence of about 0.5×10^{18} n cm^{-2} and then slightly decreases at higher fluence. The N-ZK7 follows the same general trend but shows less marked features. Its density also increases but only up to 1%. In the case of N-BK7 and S-BSL7 the opposite behaviour is observed, that is, their structure swells under neutron fluence. In fact, data shows that up to a fluence of 0.7×10^{18} n cm^{-2}, their density changes much less than the two other glasses. Above this value, their structure keeps swelling, the absolute density change surpasses that of N-ZK7.

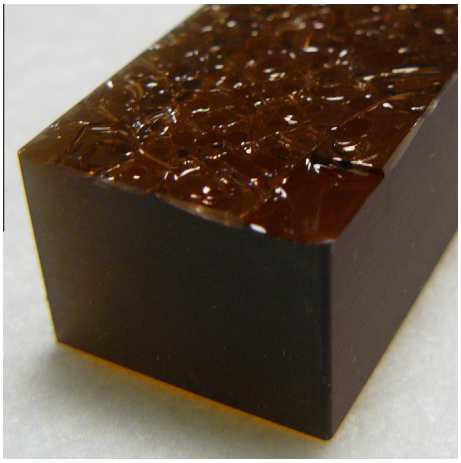

Fig. 5. Borofloat sample irradiated in H112. Irradiated surface is splintered like mosaic. The brownish colour results from the formation of large numbers of colour centers. (For interpretation of the references to colour in this figure legend, the reader is referred to the web version of this article.)

3.3. Radiation-induced plate deformation

The Neutrograph was available for our experiment only for about 23 days. Considering the frontal flux of 3×10^9 thermal-neutrons s^{-1} cm^{-2}, the fluence reached during the experiment was 6×10^{15} n s^{-1} cm^{-2} which is one fifth below the fracture limit of thick Borofloat. Therefore, we expected to be able to detect the bending of this plate. After the 23 days of ageing, one could see by the naked eye that the Borofloat plate was bent. When the non irradiated plate side was placed on a flat surface, the two edges of the plate did not touch that surface. Fig. 7 shows the raw surface signal measured by the CMM machine of the Borofloat plate.

The radii of curvature calculated from the measured curves are 37 m and 100 m for the irradiated and non irradiated plates respectively. However, one can see that the red curve drawn in Fig. 7 is quasi linear over the first and last 30 mm. From these measurements we see that the increase in density of Borofloat induces stresses when the irradiation is heterogeneous. Those stresses lead to a significant bend of the plate. For the pristine sample, the shape of the curve might be explained by residual stresses in the glass.

3.4. γ-Spectroscopy

The results of the gamma spectrometry measurements are listed in Table 6 and are given in Bq/g units. The most active glass after irradiation is N-ZK7, due to its high content of Zinc and Antimony and the long half-lives of their activation products (244.3 and 60.3 days respectively). Then come N-BK7 and S-BSL7, again with Antimony and Zinc dominating the activation products. Finally, the activity of Borofloat is mainly influenced by trace elements. The measured samples have been irradiated for 7 h with a homogeneous flux of 6.8×10^{12} n s^{-1} cm^{-2}, and the γ activity has been measured after 90 days of decay. One has to bear in mind that all the short-lived activation products such as ^{24}Na, ^{42}K, ^{31}Si that are present in hot samples, have already decayed.

Table 5
Beam fluence needed to splinter glass plate. Heterogeneous irradiation with a mean incidence angle of 4.3°. To have the sample penetrating fluence, one needs to multiply those values by sin(4.3°).

	Radiation limit (beam fluence) (n cm^{-2})	Beam number and spectrum
Brorofloat	$2.8 \times 10^{16} \pm 1.0 \times 10^{16}$	H21 – Thermal
N-ZK7	$3.7 \times 10^{17} \pm 1.3 \times 10^{17}$	H112 – Cold
N-BK7	$>2\times10^{18}$	H112 – Cold
S-BSL7	$>2\times10^{18}$	H112 – Cold

4. Discussion

4.1. Validity of radiation hardness experiments

In order to evaluate the observations of the H112/H21 experiments it becomes pertinent to carry out a combined computer simulation study using the McStas [26] code together with MCNP. The former computer package is used to simulate the beam reaching the samples whereas MCNP takes due account of the propagation of neutrons within the glass substrate and simulates the ensuing nuclear reactions. The final output yields the flux and the (n,α) reaction rate as a function of the depth within the sample. The results are finally checked out by means of an analytical estimation carried out assuming a monochromatic beam having an energy corresponding to that where the maximum intensity appears in the McStas simulation for an angle of incidence of 4.3°. Fig. 8 displays a two dimensional density plot of the beam giving the beam wavelength versus the cosine of the angle of incidence taken with respect to the normal of the sample surface. The cosine of the angle is used because it is an input parameter for neutron source orientation in MCNP.

The main results provided by the MCNP simulation are the flux and reaction rate as a function of the depth within the glass, but divided by the number of neutrons shot. The final calculation step is done by multiplying the MCNP results by the corresponding neutron intensity (λ, Cosine) and summing for each depth over the whole binning. Fig. 9 shows the results of these simulations for the Borofloat samples in H112 settings. One can see that after 250 μm of penetration, the flux and the reaction rate have been reduced by an order of magnitude. Similar simulations have been done for the other glasses. As they did not show significant differences, the corresponding plots are not drawn here.

The values quoted above are to be compared with those measured for actual guides. For such a purpose, the H522 newly installed beam has been selected. The choice of this beam to carry out such a benchmark is driven by two reasons which are:

- The H5 guide system being the latest installed guide at the ILL, it uses the most up to date neutron guide technology (coating, maximisation of the source use etc.). Hence, its geometry is probably the closest to the neutron guides that will be installed in a near future.
- Because it did not have time to age, the simulation of the beam intensity can be directly linked to measured values. In contrast, an old guide may contain a number of imperfections which are difficult to account for in the simulation. As a matter of fact, the beam intensity is affected not only by the guide geometry and source brightness, but also by the mirror degradation and the misalignments that appear from one guide element to the other.

The neutron losses have been simulated at three distances from the guide start. Table 7 summarizes the pertinent details. Figs. 10a and 10b display the dependence of the reaction rate versus penetration depth for the three guide locations just referred to.

The curves plotted in Fig. 10b show a fairly strong dependence of the reaction rate at a given depth inside the glassy substrate upon the location within the guide. The differences come from the beam energy spectrum and divergence characteristics from one position to the other. In fact, the large values shown for a

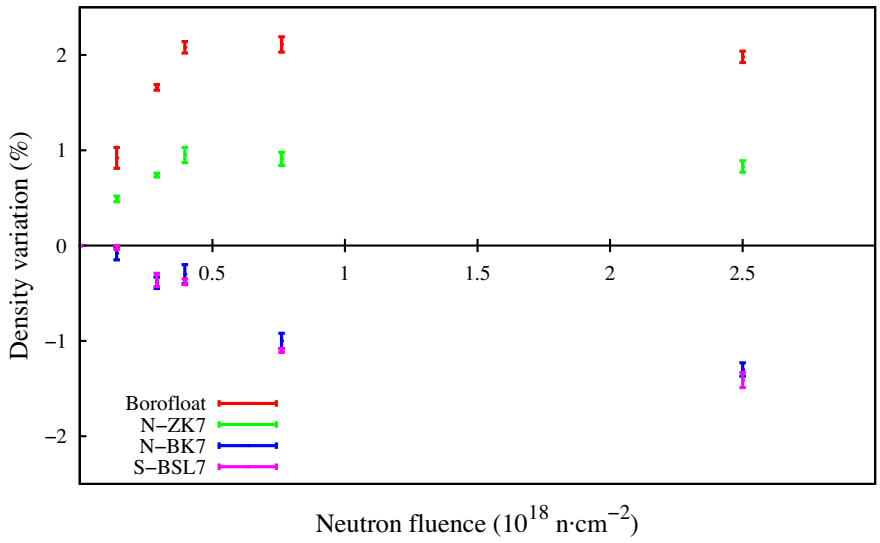

Fig. 6. Density evolution of glasses as a function received fluence. Homogeneous neutron irradiation at a temperature below 65 °C.

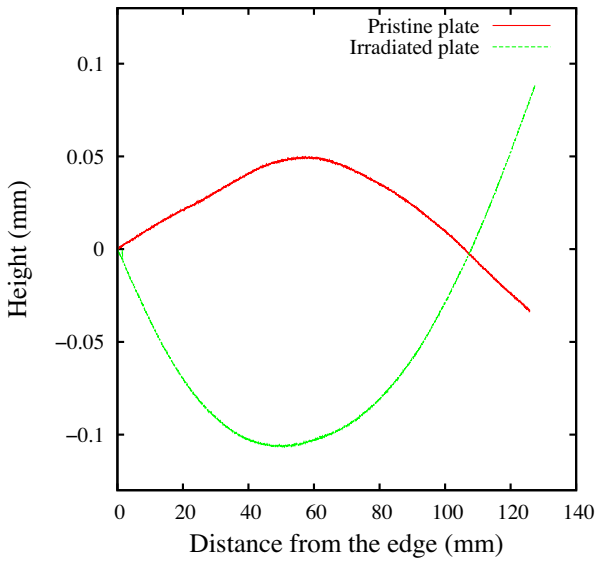

Fig. 7. Height profile of pristine and irradiated Borofloat plate.

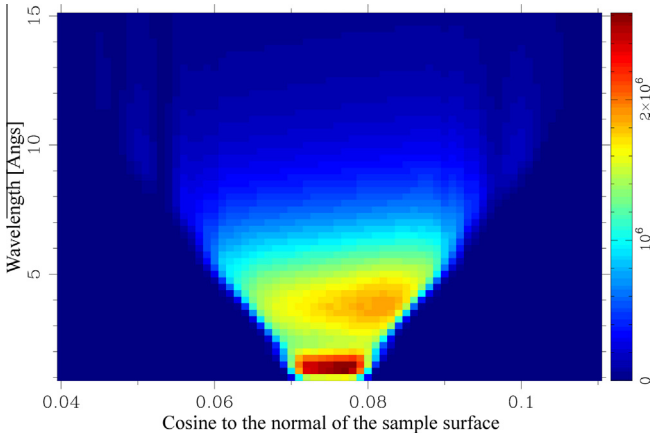

Fig. 8. Density plot of the flux on samples irradiated in H112. Wavelength and angular cosine binning.

Table 6
Main radio-nuclides detected by γ-ray-spectrometry in the samples irradiated in T4. Thermal neutron irradiation for 7 h, counting done 90 days later, values in Bq g^{-1} calculated at the end of irradiation.

Isotope	N-ZK7	N-BK7	S-BSL7	Borofloat
^{46}Sc				4.4×10^2
^{51}Cr				1.1×10^2
^{65}Zn	8.4×10^5		1.3×10^5	
^{85}Sr		3.0×10^2		
^{95}Zr/Nb				1.5×10^2
^{124}Sb	2.0×10^5	2.1×10^5	2.0×10^4	
^{131}Ba		2.2×10^2		
^{181}Hf			7.0×10^2	7.5×10^2

location closer to the reactor core such as position 1 are a direct consequence of a significantly hotter neutron energy spectrum compared to those reaching the downstream positions 2 and 3 and also having a larger beam divergence, due to a direct view of the source. Both quantities get reduced as the beam travels along the guide path which serves to filter out the more energetic neutrons and reduces the divergence. It is worth pointing out that the mean incidence angle of the H112 experiment comes closer to that of location 1 than to those for the downstream points. The strong drop in reaction rate at position 3 results from the combined effects of the decrease in the beam intensity, the smaller beam divergence as well as the colder neutron spectrum. In fact, a geometrical estimate of the direct view length $L_{\text{direct-view}} = \sqrt{8\rho a}$ given in terms of the guide radius "ρ" and width "a" yields a figure which can be compared to the distance between the guide start and the 3rd position. This means that at such guide location almost all neutrons outside of the mirror reflectivity area have been filtered out.

To give a numerical comparison between the H112 experiment and the simulation, one should bear in mind that the depth at which the reaction rate becomes 1/10 of that at the glass surface comes to be about twice the value for position 1 listed in Table 7. Notice however that such figures are small with respect to the glass plate thickness, form 10 to 15 mm. This irradiation experiment has conditions very close to those of a real guide ageing. This consolidates the values given in Table 5 as landmarks to select these materials when building new beam lines.

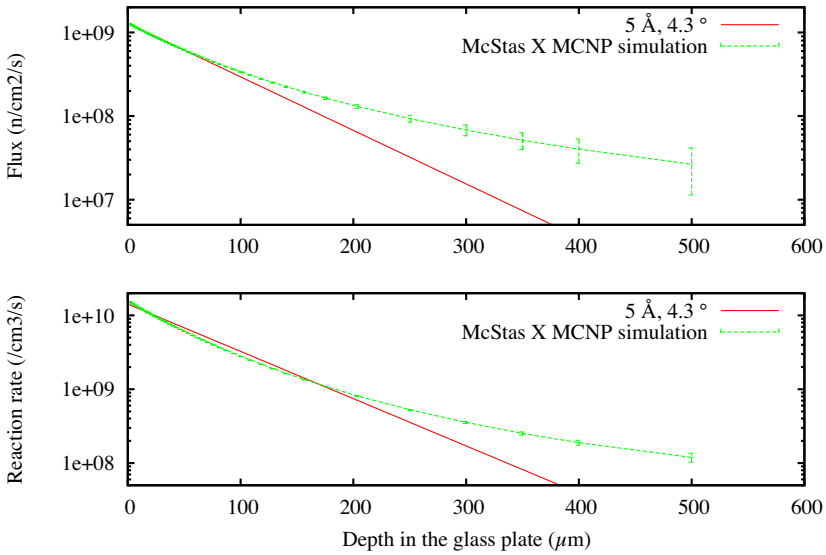

Fig. 9. Simulation and simplified analytical calculation of the flux and the reaction rate as a function of the depth in the glass substrate irradiated in H112.

Table 7
Details about the simulated H522 guide positions. The rightmost column display the depth at which the reaction rate gets down to one tenth to that shown at the glass surface.

Position	Distance from guide start (m)	Beam neutron flux ($n\,s^{-1}\,cm^{-2}$)	Reaction rate reduced to 1/10 (μm)
1	3	4.5×10^{10}	100
2	10	1.3×10^{10}	40
3	37	6.8×10^{9}	30

4.2. Considerations regarding glass density variations

Regarding the density variations upon received dose, it is pertinent to recall the pioneering studies of Simon [27], Weissman [28] and Bale [29], carried out long ago for vitreous silica under neutron radiation. Such results suggested the presence of rod-like defect clusters generated by thermal spikes within the glass matrix. The irradiation induced shrinking of amorphous SiO_2 has been correlated more recently to an increase of the small silicon ring concentration and the associated decrease of the Si–O–Si bond angle [30,31]. In contrast, further studies using a variety of radiation sources [12,32,33,14,13,34] show less marked effects on vitreous silica when irradiated with electrons and photons than those found for vitreous borosilicate. For this kind of glass, the macroscopic evolution under irradiation has also been correlated to structural changes [35]. Raman spectroscopy has shown that the Si–O–Si angle decreases with increasing dose in the case of Gold ion irradiated samples [36], which is a typical feature of the silica network. In addition, the observation of swelling of some alkali-borosilicate systems [37] has been linked to the evolution of the Boron coordination number from fourfold to threefold. Therefore, by looking at their chemical composition, it appears that Borofloat and N-ZK7, with their low alkali content, have a behaviour that could be related to that of pure silica, which results in significant shrinking. In contrast, N-BK7 and S-BSL7, with a higher network modifier concentration, show a macroscopic behaviour closer to one generally reported for borosilicate, that is swelling [15]. A deeper structural study on these glasses shall be published in the next months.

The material most prone to mechanical failure is Borofloat. In fact, inspection of Fig. 5 shows that apart from the generation of a large number of colour centers making the glass opaque, the surface displays a good number of irregularities. Such a fact has been known for some time [38] to be an unequivocal diagnose of a loss in mechanical strength. The plate bending observation is a direct observation of the stresses in the material before their release by fracture.

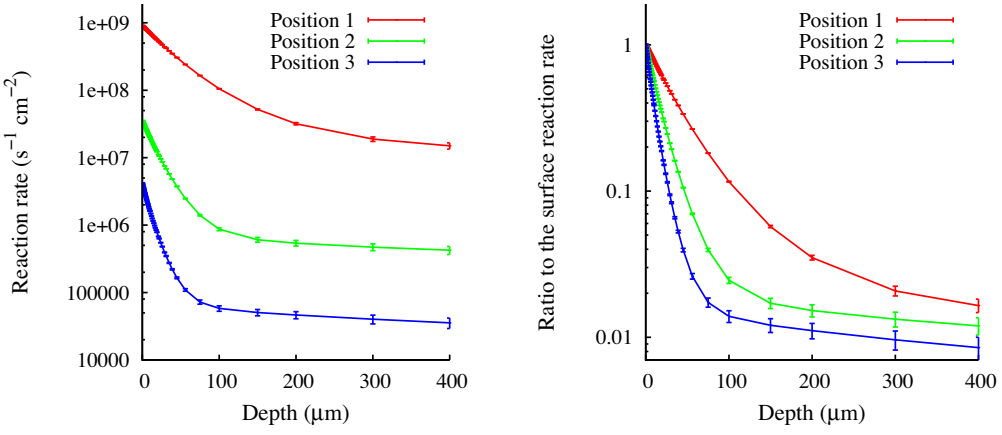

Fig. 10. Simulation of the (n,α) reaction rate as a function of the depth in the guide walls of the newly installed H522 guide. Combined McStas-MCNP simulation.

The radiation hardness limits resulting from the H112/H21 experiments may be related with the observed density variation curves. If we convert the "beam fluence" to the real fluence reaching the sample surface by multiplying the values by sin(4.3°), we see that the explored fluence in H112/H21 are below 0.5×10^{18} - n cm^{-2}. Which correspond to the high "reactivity zone" of Borofloat and N-ZK7 and the very slow swelling regime of N-BK7 and S-BSL7. Further experiments need to be carried out within this "low fluence domain", in order to explore these issues with a greater detail. These studies are planned within the ILL first reactor cycle in 2015. Anyhow the glass shrinking under the mirror for Borofloat and N-ZK7 will generate tensile stresses that lead to surface cracking. For the two other glasses such stresses are located deeper within the mirror plate. One can estimate that their fracture could occur but at much higher fluence and would initiate under the surface.

Studies on the microstructure of irradiated glasses to be carried out by means of a varied suite of experimental techniques are at present under way.

Finally, due mention should be made to efforts to develop radiation-hardened glasses mostly due to the need to equip aerospace applications with optical materials which do not lose their transmission properties with ionizing radiation [39].

5. Conclusions

The irradiation fluence limit before cracking of Borofloat and N-ZK7 has been experimentally established, while the other two examined glasses did not break during the tangential irradiation experiment. The loss of mechanical strength originates from shrinking of the glass structure, the magnitude of which is highly dependent upon the material composition. The obtained results may then be used to forecast the lifetime expectancy of future guides. Specifically in the case of Borofloat, its low irradiation resistance make it particularly unsuitable for the building of future neutron guides to operate under high flux conditions.

The analysis of the radioactive inventory carried out by γ-ray-spectrometry shows that, even if the short-lived activated products have already decayed, the use of some of the candidate materials for glass substrates such as N-ZK7, should be planned with care due to the relatively high amount of long-lived radioisotopes generated.

Finally it is worth remarking that although some radiation hardened glasses have been developed for aerospace and inertial fusion applications, such materials are not considered as realistic candidates for guide manufacturing due to their high cost.

Acknowledgements

We thank the guide manufacturers for the assistance they provided all along this study. Romain Boffy acknowledges financial support from the ESS-Bilbao Consortium.

Finally, the study here exposed would not have been possible without the combined efforts of ILL staff throughout several years, specially the SMAE, BPC, Bloc-Pile and Radio-Protection services. The authors thank them for their constant support.

References

[1] D. Hughes, M. Burgy, Reflection of neutrons from magnetized mirrors, Phys. Rev. 81 (1951) 498.
[2] H. Maier-Leibnitz, T. Springer, The use of neutron optical devices on beam-hole experiments, J. Nucl. Energy A/B 17 (1963) 217–225.
[3] B. Alefeld, J.C.C. Kukla, D. Scherm, W. Schmatz, Jülich Rep. 294 (1965).
[4] Joint Meeting of the National Organization of Test, Research, and Training Reactors and the International Group on Research Reactors, Analysis of the Causes and Consequences of Neutron Guide Tube Failures. URL http://www.ncnr.nist.gov/trtr2005/Proceedings/Rowe%20-%20Consequences%20of%20Guide%20Failure.pdf
[5] J. Beaucour, D. Bazzoli, R. Gaehler, M. Kreuz, A. Perillo-Marcone, P. Thomas, Do neutron guides live forever?, in: 1st Neutron Delivery System Workshop, 2006.
[6] P. Link, Neutron guides, not always perfect, FRM II News 8 (2012) 10.
[7] S. Pullen, G. Davidson, S. Pangalis, F. Klose, S. Kennedy, Report on the repair of the opal neutron beam transport system, in: Joint IGORR 2013 and IAEA Technology Meeting, 2013, URL https://inis.iaea.org/search/searchsinglerecord.aspx?recordsFor=SingleRecord&RN=45103462.
[8] B. Ballot, Étude par réflectivité de neutrons de multicouches métalliques Nickel/Titane pour miroirs de neutrons, Ph.D. thesis, Université Paris XI, 1995.
[9] K. N'Guy Maréchal, Tenue sous irradiation de supermiroirs pour guides de neutrons, Ph.D. thesis, Université Paris XI, 1997.
[10] J. Paymal, M. Bonnaud, Modification des verres sous l'influence des rayonnements, in: Journées internationales d'études 1961 de l'Association belge pour favoriser l'étude des Verres et des Composés siliceux, 1961, pp. 17–31.
[11] P. Ageron, Bauer, P. Blum, C. Bouton, J. Brown, Bureau, Faudou, J. Joffrin, R. Mathieu, T.S.M. Thomas, Wheeler, J. White, Meeting report, ILL internal communication, 1978 (December).
[12] B. Gross, Irradiation effects in borosilicate glass, Phys. Rev. 107 (1957) 368.
[13] N. Baydogan, A. Tugrul, Borosilicate glass for gamma irradiation fields, Solid State Sci. 14 (2012) 1692–1697.
[14] A. Abbas, Y. Serruys, D. Ghaleb, J. Delaye, B. Boizot, B. Reynard, G. Calas, Nucl. Instr. Meth. Phys. Res. B 166–167 (2000) 445–450.
[15] S. Peuget, J.-N. Cachia, C. Jégou, X. Deschanels, D. Roudil, V. Broudic, J.-M. Bart, Irradiation stability of R7T7-type borosilicate glass, J. Nucl. Mater. 354 (2006) 1–13.
[16] S. Sato, H. Furuya, T. Kozada, Y. Inagaki, T. Tamai, Volumetric change of simulated nuclear waste glasses irradiated by the $^{10}B(n,\alpha)^{7}Li$ reaction as simulation of actinide irradiation, J. Nucl. Mater. 152 (2–3) (1988) 265–269.
[17] S. Peuget, T. Fares, E. Maugeri, R. Caraballo, T. Charpentier, L. Martel, J. Somers, A. Janssen, T. Wiss, F. Rozenblum, M. Magnin, X. Deschanels, C. Jégou, Effect of ^{10}B (n,α)Li irradiation on the structure of a sodium borosilicate glass, Nucl. Instr. Meth. Phys. Res. B 327 (2014) 22–28.
[18] W.J. Weber, R.C. Ewing, C.A. Angell, G.W. Arnold, A.N. Cormak, J.M. Delaye, D.L. Griscom, L.W. Hobbs, A. Navrotsky, D.L. Price, A.M. Stoneham, M.C. Weinberg, Radiation effects inglasses used for immobilization of high-level waste and plutonium disposition, J. Nucl. Mater. 12 (8) (1997) 1946–1978.
[19] S. Peuget, J.-M. Delaye, C. Jégou, Specific outcomes of the research on the radiation stability of the french nuclear glass towards alpha decay accumulation, J. Nucl. Mater. 444 (2014) 76–91.
[20] J. Beaucour, in: 2nd Neutron Delivery System Workshop, 2009.
[21] Los Alamos National Laboratory, MCNP6.1. URL https://laws.lanl.gov/vhosts/mcnp.lanl.gov/index.shtml.
[22] J. Ziegler, J. Manoyan, The stopping of ions in compounds, Nucl. Instr. Meth. Phys. Res. B 35 (1988) 215–228.
[23] M. Soutif, Physique Neutronique, Presses Universitaires de France, 1962.
[24] A. Van-Overberghe, High flux neutron imaging for highly dynamic and time resolved non-destructive testing, Ph.D. thesis, University of Heidelberg, 2006.
[25] C.L. Allred, J.T. Borenstein, L.W. Hobbs, Neutron irradiation-induced dimensional changes in mems glass substrates, Nucl. Instr. Meth. Phys. Res. B 264 (2007) 66–72.
[26] P. Willendrup, E. Farhi, K. Lefmann, Mcstas 1.7 – a new version of the flexible monte carlo neutron scattering package, Phys. B Condens. Matter (Amsterdam, Netherlands) 350 (2004) 735–737.
[27] I. Simon, Structure of neutron-irradiated quartz and vitreous silica, J. Am. Ceram. Soc. 40 (5) (1957) 150–153.
[28] S. Weissmann, K. Nakajima, J. Appl. Phys. 34 (1963) 611.
[29] H. Bale, R. Shepler, G. Gibbs, J. Appl. Phys. 41 (1970) 241.
[30] R. Devine, Macroscopic and microscopic effects of radiation in amorphous SiO_2, Nucl. Instr. Meth. Phys. Res. B 91 (1994) 378–390.
[31] J.-M. Delaye, S. Peuget, G. Bureau, G. Calas, Molecular dynamics simulation of radiation damage in glasses, J. Non-crystal. Solids 357 (14) (2011) 2763–2768.
[32] M. Antonini, A. Manara, S. Buckley, Microstructural changes in irradiated silica based glasses, Radiat. Effects 65 (1982) 55–61.
[33] M. Sacchi, M. Anttonini, S. Buckley, A. Manara, Alkali effects on bubble formation in irradiated borosilicate glasses, Mater. Lett. 4 (1) (1985) 10–12.
[34] K. Yang, T. Wang, G. Zhang, H. Peng, L. Chen, L. Zhang, C. Li, F. Tian, W. Yuan, Study of irradiation damage in borosilicate glass induced by he ions and electrons, Nucl. Instr. Meth. Phys. Res. B 307 (2013) 541–544.
[35] S. Peuget, E.A. Maugeri, T. Charpentier, C. Mendoza, M. Moskura, T. Fares, O. Bouty, C. Jégou, Comparison of radiation and quenching rate effects on the structure of a sodium borosilicate glass, J. Non-Crystal. Solids 378 (2013) 201–212.
[36] J. De Bonfils, S'Peuget, G. Panczer, D. de Ligny, S. Henry, P.-Y. Noël, A. Chenet, B. Champagnon, Effect of chemical composition on borosilicate glas behavior under irradiation, J. Non-Cryst. Solids 356 (6–8) (2010) 388–393.
[37] C. Mendoza, S. Peuget, T. Charpentier, M. Moskura, R. Caraballo, O. Bouty, A. Mir, I. Monnet, C. Grygiel, C. Jegou, Oxide glass structure evolution under swift heavy ion irradiation, Nucl. Instr. Meth. Phys. Res. B 325 (2014) 54–65.
[38] G.M. Bartenev, Strength and Mechanisms of Fracture of Polymers, 1984 (Moscow).
[39] A.I. Gusarov, D. Doyle, A. Hermanne, F. Berghmans, M. Fruit, G. Ulbrich, M. Blondel, Refractive-index changes caused by proton radiation in silicate optical glasses, Appl. Opt. 41 (4) (2002) 678–684.